Calculation of the Via-Plate Capacitance of a Via with Pad Using Finite Difference Method for Signal/Power Integrity Analysis

Yaojiang Zhang #1, Erping Li #2, Xianke Gao #3, Arun Reddy Chada *4, Jun Fan *5

Computational Electronics and Photonics, Institute of High Performance Computing, Singapore
#1,2,3 *{zhangyj, eplee, gaoxk}@ihpc.a-star.edu.sg*
* *EMC laboratory, Missouri University of Science & Technology (former University of Missouri-Rolla), MO 65401, USA*
*4,5 *{ac253, jfan}@mst.edu*

Abstract— **Finite difference method is used to calculate the via-plate capacitances for vias with pad. Due to the symmetric structure, the solving domain is reduced to a rectangular $\rho - z$ region. Boundary conditions along the region are discussed. Both barrel-plate and pad-plate capacitances are studied with various geometric parameters. The results could be used as validations for possible analytical expressions of these capacitances.**

I. INTRODUCTION

Vias are widely used, tinny structures connecting traces and planes in different layers of a multilayer printed circuit boards or packages. As an inevitable discontinuities along traces and sources for simultaneous switching noise along power/ground planes, accurate model for vias is critical for both signal integrity and power integrity analyses.

The parasitic capacitance between a via and the surrounding plate has been extensively studied using both numerical and analytical analysis [1]-[3]. However, these studies are usually for a via crossing a single plate, and the parasitic capacitance is called 'excess capacitance' used in a π-type circuit model for the via lumped circuit model.

Recently, a physics-based via circuit model is proposed for signal link path analysis and its feasibility has been demonstrated[4][5]. In this model, a via is represented as a π-type circuit where the via barrel is a short circuit; two via-plate capacitances are used to describe the displacement current from the via barrel to top/bottom planes and the impedance between two planes is used to denote the return current path. The impedance of parallel planes has been extensively studied. On the other hand, an analytical formula has been derived for the evaluation of the via-plate capacitance. Formula in [6], however, is only valid for those vias without a pad, *i.e.* with same barrel and pad radius.

In this paper, quasi-static finite difference method (FDM) is used to calculate the via-plate capacitance for the vias with different pad and barrel radius. Due to the symmetry of the via circular structure, the solving domain is reduced to a two dimensional rectangular region. The impact of the pad on the via-plate capacitance will be discussed. It will also provide a validation tool for the possible analytical expression for a via with pad.

II. THE NUMERICAL METHOD FOR THE BARREL-PLATE CAPACITANCE OF A VIA WITH PAD

Fig. 1 shows a via with pad crossing two parallel planes. The barrel, pad and anti-pad radii are r, a and b, respectively. The separation of two planes is h. Between the planes is the dielectric material with a permittivity of ε_r. Due to the reason discussed in [5] and [6], the middle surface between two planes as shown in Fig. 1 satisfies the boundary condition of a perfect magnetic conductor (PMC). Moreover, the circular symmetry of the via structure can further reduce the solving domain into a rectangular region in $\rho - z$ plane where $\rho \in [r, R]$ and $z \in [0, h/2]$ as shown in Fig.2. The artificial boundary $\rho = R$ is chosen to terminate the solving domain. Since the static field decay inversely from sources, the final capacitance would converge when $\rho = R$ is far away from the anti-pad. From our simulation , $R \geq 3\max\{b, h\}$ is a practical selection for acceptable simulation.

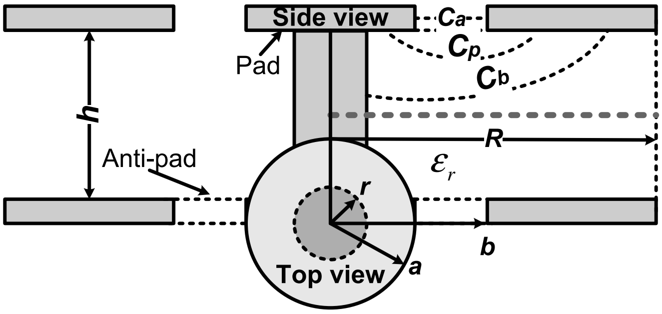

Fig. 1. Geometry of a via crossing a plane pair.

Fig. 2 indicates that for a via with a pad, there not only has the barrel-plate capacitance C_b but also the pad-plate capacitance C_p. The total capacitance from the via to the plate should be the summation of C_b and C_p. The coaxial capacitance C_a can be obtained using analytically as the transverse electromagnetic mode is assumed in the anti-pad. Therefore, only C_b and C_p are discussed here.

Copyright © 2009 IEICE

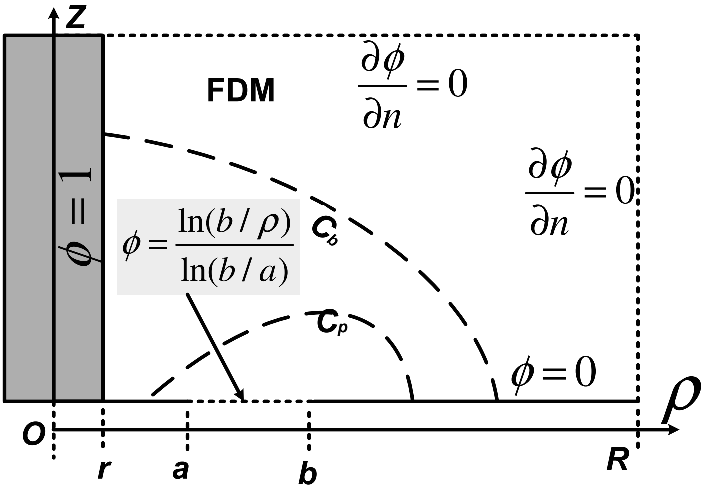

Fig. 2. Computational domain and the boundary conditions for finite difference method.

The potential ϕ distributed in the solving domain satisfies the following Laplace equation for axis-symmetric structure [4]

$$\frac{1}{\rho}\frac{\partial}{\partial\rho}\left(\rho\frac{\partial\phi}{\partial\rho}\right)+\frac{\partial^2\phi}{\partial z^2}=0 \tag{1}$$

and the boundary conditions at the solving domain are specified as shown in Fig. 2 that

$$\phi=1 \quad \{\rho=r, z\in[0,h/2]\}\bigcup\{\rho\in[r,a], z=0\}; \tag{2}$$
$$\frac{\partial\phi}{\partial n}=0 \quad \{\rho\in[0,R], z=h/2\}\bigcup\rho=R, z\in[0,h/2]; \tag{3}$$
$$\phi=0 \quad \rho\in[b,R], z=0; \tag{4}$$
$$\phi=\frac{\ln(b/\rho)}{\ln(b/a)} \quad \rho\in[a,b], z=0. \tag{5}$$

Notice that the boundary condition of (5) is used for the potential in the anti-pad, as the transverse electromegnetic mode is assumed in the anti-pad. Our experience shows that this can speed up the convergence comparing with the case using Neumann boundary in the anti-pad, especially for the vias with pad.

Following the conventional finite difference scheme, the differential equation in (1) can be discretized into following difference equations

$$\phi_{i,j}=A\phi_{i+1,j}+B\phi_{i-1,j}+C\phi_{i,j+1}+D\phi_{i,j-1} \tag{6}$$

where subscript i,j denotes the grid index for each node, and the coefficients are obtained by

$$A = \left[\frac{1}{(\Delta\rho)^2}+\frac{1}{2\rho_{i,j}\Delta\rho}\right]/F \tag{7}$$
$$B = \left[\frac{1}{(\Delta\rho)^2}-\frac{1}{2\rho_{i,j}\Delta\rho}\right]/F \tag{8}$$
$$C = \frac{1}{(\Delta z)^2}/F \tag{9}$$
$$D = \frac{1}{(\Delta z)^2}/F \tag{10}$$
$$F = \frac{1}{(\Delta\rho)^2}+\frac{1}{(\Delta z)^2} \tag{11}$$

where $\Delta\rho$ and Δz are grid steps along ρ and z directions, respectively. When $\Delta\rho=\Delta z=h$, *i.e.* same grid step is selected for both ρ and z directions, the difference scheme in (6) can be simplified as

$$\begin{aligned}\phi_{i,j} &= \frac{1}{4}(\phi_{i+1,j}+\phi_{i-1,j}+\phi_{i,j+1}+\phi_{i,j-1})+\\ &\quad \frac{h}{8\rho_{i,j}}(\phi_{i+1,j}+\phi_{i-1,j})\end{aligned} \tag{12}$$

Although (6) is more general difference scheme, the simplified one of (12) is adopted in this paper. The potential value at each grid point is renewed in each iteration using (12). The iteration will stop when all the potentials become stable according to a specified criterion. The charge density along the via barrel and pad can be calculated as

$$\sigma_e=-\varepsilon_r\varepsilon_0\nabla\phi\cdot\mathbf{n} \tag{13}$$

where $\mathbf{n}$ is the normal vector on the via barrel and pad. The barrel-plate capacitance C_b and the pad-plate capacitance C_p are the charges along the via barrel and pad, respectively. Then we have

$$C_b = -\varepsilon_r\varepsilon_0\int_0^{h/2}2\pi r\frac{\partial\phi}{\partial\rho}|_{\rho=r}dz \tag{14}$$
$$C_p = -\varepsilon_r\varepsilon_0\int_r^{a}2\pi\rho\frac{\partial\phi}{\partial z}|_{z=0}d\rho \tag{15}$$

where the differential operators can be replaced by the difference ones in numerical calculations.

III. NUMERICAL EXAMPLES AND DISCUSSIONS

The finite difference method can solve the vias with or without pad. The via-plate capacitance for the vias without pad is calculated to validate the implementation of the method (Matlab programming language is used) as both numerical and analytical data are available in [6]. Fig. 3 shows the iteration convergence in solving the difference equations for an example of a via without pad. It can be seen that different meshing grid steps results in different convergence rate. For sparse mesh grid (0.20 mil), it only takes less than 2000 iteration steps to get a stable but not very accurate value. On the other hand, for the fine mesh case (0.05 mil), it requires at least 16,000 steps to converge, which is too time consuming. Therefore, there is a balance between the accuracy and efficiency for the via capacitance calculation using FDM. In the following

Copyright © 2009 IEICE

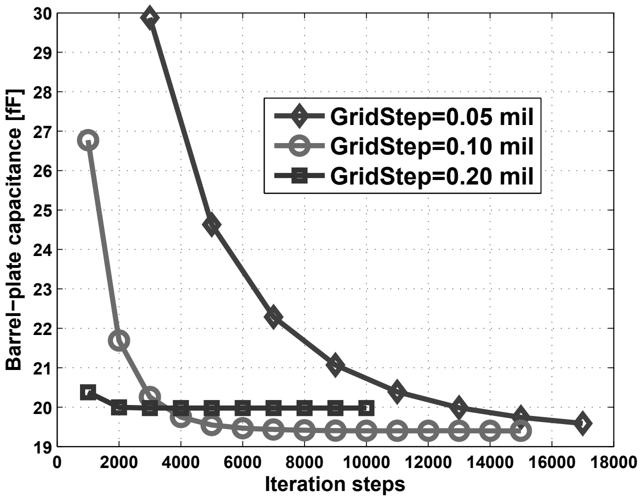

Fig. 3. Convergence of the barrel-plate capacitance calculation using the finite difference method. ($r = a = 4, b = 14, h = 4.5, \text{Unit : mil}; \varepsilon_r = 3.84$)

simulations, the meshing grid step is selected to be 0.1 mil and the iteration number is set to be 7000.

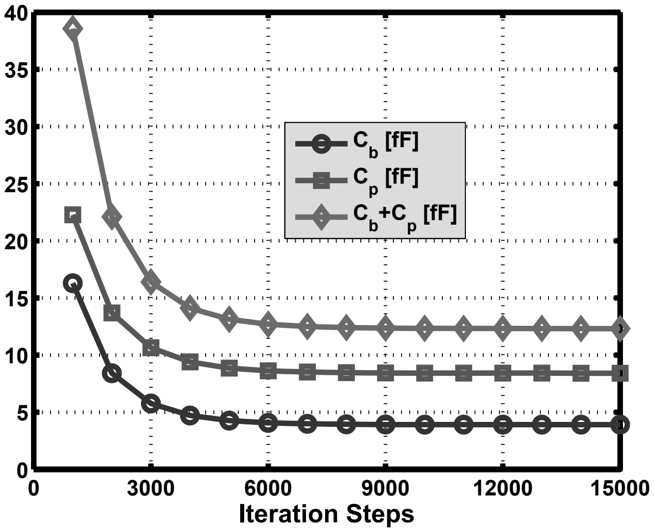

Fig. 4. Convergence of the barrel-plate, the pad-plate and total via capacitances (C_b, C_p and $C_b + C_p$. ($r = 4, a = 8, b = 20, h = 4.5, \text{Unit : mil}; \varepsilon_r = 3.84$)

TABLE I

COMPARISON OF THE CONCENTRIC VIA-PLATE CAPACITANCE VALUE CALCULATED BY ELECTROSTATIC SOLVER, CST EM STUDIO, THE ANALYTICAL FORMULA OF [6] AND THE FDM PROPOSED HERE ($h_u = h_d$=0.2286 MM (9 MILS), t=0.0254 MM (1 MIL); $\varepsilon_r = 3.84$.)

case	radii (mm)		C_{via} (fF) (Elapsed time:seconds)		
	a	b	CST EM Studio	[6]	FDM
1	0.1016	0.3556	40.7 (303)	42.6 (0.15)	43.2 (27.8)
2	0.1016	0.4318	36.2 (301)	37.2 (0.15)	37.7 (34.4)
3	0.1016	0.5080	32.8 (308)	33.4 (0.15)	34.1 (41.2)
4	0.1524	0.3556	58.2 (380)	61.7 (0.15)	62.9 (26.0)
5	0.1524	0.4318	48.9 (365)	51.2 (0.15)	52.3 (33.1)
6	0.1524	0.5080	43.2 (308)	44.6 (0.15)	45.6 (39.2)
7	0.2032	0.3556	84.7 (431)	89.6 (0.15)	91.6 (24.8)
8	0.2032	0.4318	66.1 (425)	69.9 (0.15)	71.5 (30.7)
9	0.2032	0.5080	55.7 (365)	58.4 (0.15)	59.7 (38.1)

Table. I compares the via-plate capacitances obtained by the 3-D commercial software (CST EM Studio), the analytical formula as well as the 2-D finite difference method here. It can be seen that the results from FDM with 7000 iteration steps agree very well with the results using the analytical solutions (less than 3% differences). Moreover, the 2D FDM is much faster than the 3D commercial electro-static solver although it is very slower than the analytical formula derived in [6]. These examples demonstrate the accuracy of the FDM implementation.

Fig. 4 gives an example of the iteration convergence of the FDM for a via with pad. Both the barrel-plate and pad-plate capacitances (C_b and C_p) decrease and converges to stable values with the increase of iteration steps.

Fig. 5 compares the trends of C_b and C_p with different pad radius a with fixed other parameters such as the barrel, pad and anti-pad radii r, b and b. It can be seen that in the case of $a = r$, there is no pad-plate capacitance *.i.e.* $C_p = 0$. With the increase of the pad radius, C_p increases while C_b decreases steadily. The total via capacitance first decreases with pad radius and then increases as pad radius becomes larger and larger.

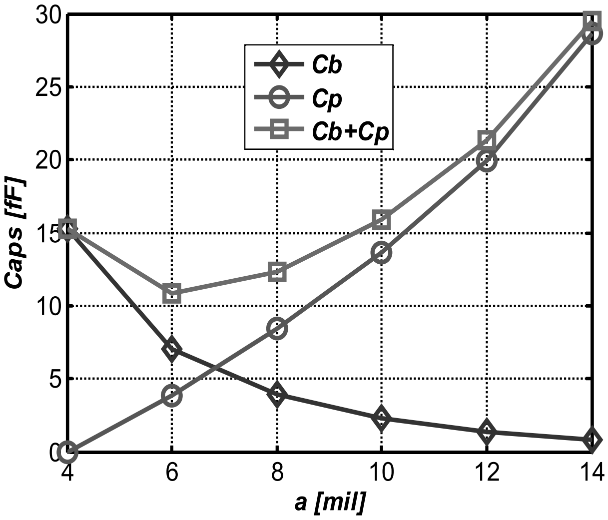

Fig. 5. The barrel-plate and pad-plate capacitances versus the pad radius with fixed other geometries. ($r = 4, b = 20, h = 4.5, \text{Unit : mil}; \varepsilon_r = 3.84$)

Fig. 6 presents the different variations of barrel-plate and pad-plate capacitances with the separation of plates. Interestingly, the pad-plate capacitance C_p quickly reaches a maxi-

Copyright © 2009 IEICE

mum value when the via height or late separation h is larg enough. On the other hand, the barrel-plate capacitance C increase almost linearly with the plate separation h. In th case of small plate separation, C_p dominates the via-plat capacitance while in the case of large plate separation, C is the main part of the parasitic capacitances from the via t the plate.

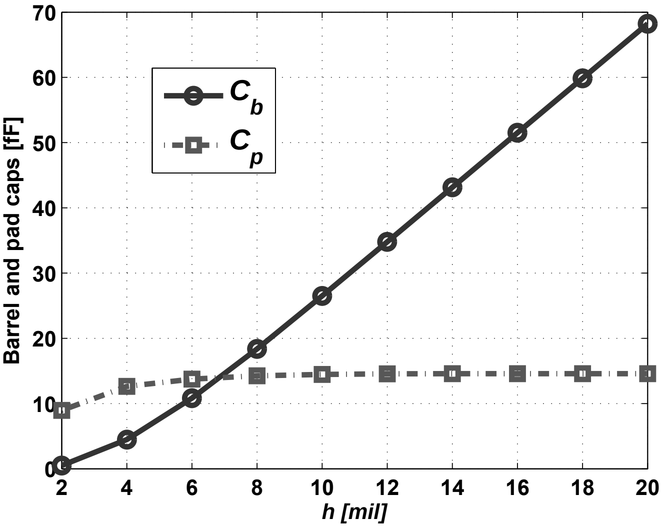

Fig. 6. The barrel-plate and pad-plate capacitances versus the plate sepa tions with fixed other geometries. ($r = 4, a = 8, b = 20, \text{Unit : mil}; \varepsilon_r$ 3.84)

The potential distributions for a via without and with a pa have been depicted in Fig. 7 (a) and (b) respectively. For thes two examples, the potentials change rapidly in the anti-pa region and its extension region along z-directions. For a vi with pad, Fig. 7 (b) shows that the potentials near the ant pad have more complicated contours. This means that the pa radial extension causes complex electric field distributions.

IV. CONCLUSIONS

Finite difference method is used to extract the via-plate capacitance for vias with pad by solving electro-static equations. The boundary conditions are specified in the anti-pad and artificial boundaries are set to terminate the computational domain. Accuracy and efficiency have been discussed by comparing with the analytical formula for vias without pad. Variations of the parasitic capacitances with geometric parameters are investigated. Moreover, it can also be used as validations for other extraction approaches for the vias with pad.

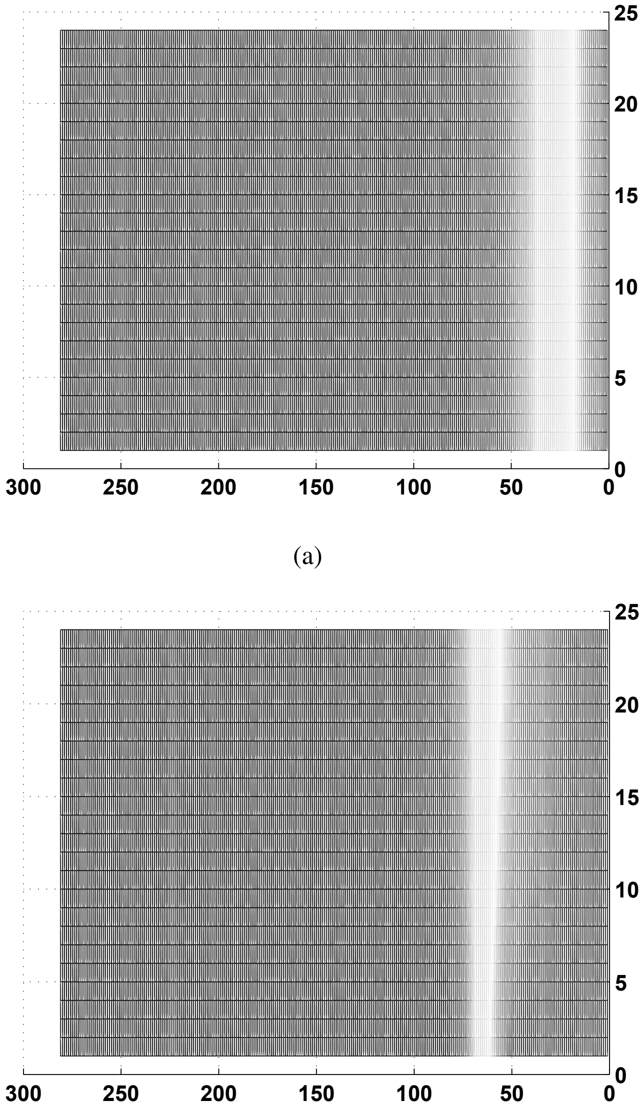

(a)

(b)

Fig. 7. Potential distributions for a via (a) without ($r = a = 4$) and (b) with a pad ($r = 4, a = 14$). ($b = 20, h/2 = 4.5, \text{unit : mil}; \varepsilon_r = 3.84$)

REFERENCES

[1] T. Wang, R. F. harington, and J. R. Mautz, "Quasi-Static analysis of a microstrip via through a hole in a ground plane, " *IEEE trans. Microwave Theory Tech.,* vol. 36, no. 6, pp.1008-1013, Jun 1988.

[2] P. Kok, and D. De Zutter, "Capacitance of a circular symmetric model of a via hole including finite ground plane thickness," *IEEE Trans. Microwave Theory Tech.*, vol. 39, no. 7, pp. 1229-1234, July 1991.

[3] P. A. Kok, and D. D. Zutter, "Prediction of the excess capacitance of a via-hole through a multilayered board including the effect of connecting microstrips or striplines, " *IEEE Trans. Microwave Theory Tech.*, vol. 42, no. 12, pp. 2270-2276, Dec. 1994.

[4] C. Schuster, Y. Kwark, G. Selli, and P. Muthana, "Developing a 'Physical' Model for Vias," DesignCon 2006, Santa Clara, CA USA, Feb. 6 - 9, 2006.

[5] G. Selli, C. Schuster, Y. H. Kwark, M. B. Ritter, and J. L. Drewniak, "Developing a Physical Via Model for Vias - Part II: Coupled and Ground Return Vias", DesignCon 2007, Santa Clara, CA USA, Jan. 29 - Feb. 1, 2007.

[6] Y. Zhang, J. Fan, G. Selli, M. Cocchini, F. D. Paulis, "Analytical evaluation of via-plate capacitance for multilayer printed circuit boards and packages, " *IEEE Trans. Microwave Theory Tech.,* vol. 56, no. 9, pp. 2118-2128, Sep 2008.

Copyright © 2009 IEICE